ADA034224

IGNITION AND PROPAGATION RATES
FOR FLAMES IN A FUEL MIST

C. E. Polymeropoulos
V. Sernas

NOVEMBER 1976

FINAL REPORT

Document is available to the public through the
National Technical Information Service
Springfield, Virginia 22151

Prepared for

U. S. DEPARTMENT OF TRANSPORTATION
FEDERAL AVIATION ADMINISTRATION
Systems Research & Development Service
Washington, D.C. 20590

NOTICE

This document is disseminated under the sponsorship
of the Department of Transportation in the interest of
information exchange. The United States Government
assumes no liability for its contents or use thereof.

1. Report No.	2. Government Accession No.	3. Recipient's Catalog No.
FAA-RD-76-31		

4. Title and Subtitle	5. Report Date
IGNITION AND PROPAGATION RATES FOR FLAMES IN A FUEL MIST.	November 76
	6. Performing Organization Code

7. Author(s)	8. Performing Organization Report No.
C. E. Polymeropoulos and V. Sernas	FAA-NA-76-162

9. Performing Organization Name and Address	10. Work Unit No. (TRAIS)
Federal Aviation Administration National Aviation Facilities Experimental Center Atlantic City, New Jersey 08405	
	11. Contract or Grant No.
	131-520-060

12. Sponsoring Agency Name and Address	13. Type of Report and Period Covered
U.S. Department of Transportation Federal Aviation Administration Systems Research and Development Service Washington, D. C. 20590	Final Report, January 1975-January 1976
	14. Sponsoring Agency Code

15. Supplementary Notes   Tests performed and report prepared by Department of Mechanical, Industrial and Aerospace Engineering, Rutgers, The State University of New Jersey, New Brunswick, New Jersey 08903

16. Abstract

The droplet size distribution in various experimental air-fuel sprays was measured using a holographic method. There was good agreement between upper-limit log-normal velocity distribution functions and the droplet size data. The Sauter mean diameter, maximum droplet diameter, and air-fuel ratio were also well represented by the data. Measurements of burning velocities in the sprays tested were compared with calculated predictions, and the results were satisfactory. Approximate burning velocities in modified fuel sprays produced under wind shear conditions were also calculated.

17. Key Words	18. Distribution Statement
Fuels Holography Sprays Burning Velocity	Document is available to the public through the National Technical Information Service, Springfield, Virginia, 22151

19. Security Classif. (of this report)	20. Security Classif. (of this page)	21. No. of Pages	22. Price
Unclassified	Unclassified	55	

Form DOT F 1700.7 (8-72)   Reproduction of completed page authorized

240 550

PREFACE

This report was prepared by the Mechanical, Industrial and Aerospace Engineering Department at Rutgers, The State University of New Jersey, for the Federal Aviation Administration. The work was performed from January 1975 to January 1976 under the management of Mr. S. Zinn, from the Fire Protection Branch, Aircraft and Airport Safety Division, National Aviation Facilities Experimental Center, Atlantic City, New Jersey.

Messrs. D. Jones and A. Veninger assisted in the design of the experimental apparatus, as well as the collection of the experimental data at Rutgers.
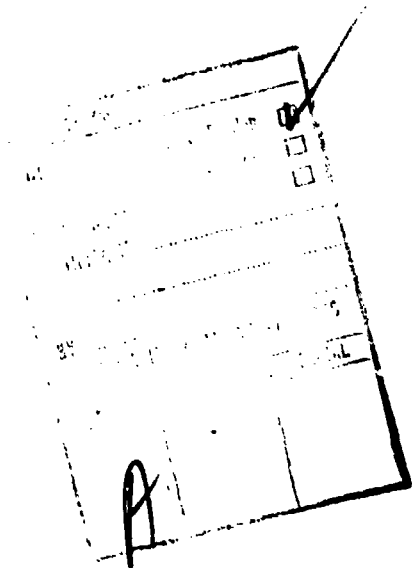
TABLE OF CONTENTS

LIST OF ILLUSTRATIONS

LIST OF TABLES

LIST OF ABBREVIATIONS AND SYMBOLS

a	constant in upper limit log-normal droplet size distribution
(A/F)	air to fuel ratio measured at the tube exit
$(A/F)_\ell$	air to fuel mass ratio based on the measured liquid volume
$(A/F)_c$	air to fuel ratio calculated from the droplet counts
c_p	specific heat at constant pressure for air
$c_{p\ell}$	specific heat of the liquid fuel
d	droplet diameter in holographic work
D	droplet diameter
D_i	diameter of group size i in droplet distribution
D_m	maximum droplet diameter in droplet size distribution
D_{32}	$\sum\limits_i N_i D_i^3 / \sum\limits_i N_i D_i^2$
$(F/A)_\ell$	fuel to air mass ratio based on the measured liquid volume
$(F/A)_v$	fuel to air mass ratio based on the calculated vapor mass fraction
h	heat transfer coefficient
k	thermal conductivity of air
L	fuel latent heat of vaporization
$\dot{m}$	evaporation rate
$\dot{m}_c$	evaporation rate from a spray with cylindrical shaped particles
$\dot{m}_s$	evaporation rate from a spray with spherical particles
M	molecular weight of the gas mixture
M_F	molecular weight of the fuel
N	$\lambda_1 Z_1 / d^2$
N_i	number of droplets in diameter range i
N_u	Nusselt number (hD/k)
N_1, N_2	droplet counts from two holograms 1 and 2
n	number of droplets per unit volume
n_c	number of cylindrical particles per unit volume
r	radial distance from tube axis
R	tube radius
R_e	Reynolds number
T_∞	ambient temperature
T_s	temperature at the droplet surface
T_B	fuel boiling point
t	time
u	speed of mixture in the x-direction
u'	rms velocity fluctuations
v	cumulative volume fraction of droplets in the spray
v_T	total estimated liquid volume obtained from droplet size distributions
V_a	mean air velocity
V_i	terminal velocity of droplets of size i
V_s	volume scanned for the droplet counts
V_{si}	liquid volume in size range i

x	downstream distance
y	$\ln\left(\dfrac{aD}{D_m - D}\right)$
z_1	holographic recording distance
z_2	reconstruction distance

Greek Symbols

δ	constant in upper-limit log-normal droplet size distribution
η	cumulative numerical size distribution
λ	wavelength of light
λ_1	wavelength of recording light
λ_2	wavelength of reconstructing light
μm	micro-meters
ρ	mixture density
ρ_a	air density
ρ_s	defined in equation (5)
ρ_ℓ	liquid density

INTRODUCTION

PURPOSE.

The purpose of the research effort described in this report was
to (a) develop a holographic method for the measurement of droplet
sizes in sprays, (b) to employ this method for the measurement of
size distributions in sprays of various air-fuel ratios, as well
as for elevated upstream temperature conditions and to relate the
droplet size distributions to measured values of burning veloci-
ties, (c) to carry out calculations of burning velocities in modi-
fied fuel sprays produced by air shear atomization in an air flow
facility, and (d) to incorporate in the model used for the burning
velocity calculations, physical behavior ta of modified fuel
sprays, as it became available from the work currently being
carried out at the Jet Propulsion Laboratory, in Pasadena,
California.

Except for task (d) above, all other tasks were carried out, and
the results are described in the present report. Task (d) was not
performed because no information relevant to the burning velocity
of modified fuels became available during the period of this con-
tract.

BACKGROUND

Previous work under the present contract has appeared in refer-
ences 1, 2 and 3. These describe in detail the model calculations
of the burning velocity in air fuel sprays, as well as the initial
experiments that were carried out to measure burning velocities in
polydisperse kerosene-air sprays. The results described in refer-
ences 1 to 3 point to the importance of the droplet size and of
the air-fuel ratio on the burning velocity. In addition, the
calculated predictions of reference 1 point to the sensitivity
of the burning velocity on the upstream mixture temperature.

The experimental portion of the work carried out at Rutgers Uni-
versity, was aimed at producing accurate data for checking the
predictive capability of the model which was developed for the
calculation of burning velocities in sprays. In addition, mea-
surements carried out at elevated air temperatures were also com-
pared with similar results obtained using the spray model. The
effect of ambient air temperature on burning velocity is impor-
tant for aircraft fire safety, since mists or sprays, can be
formed during crashes occurring in hot or cold weather.

Attempts at measuring the burning velocity of modified fuel
sprays using the experimental apparatus employed for the testing
of neat fuels did not prove successful. This was because the re-
sulting mixture consisted of particles which were too widely

1

spaced for sustaining a continuous combustion wave.

The model developed for the calculation of burning velocities in
sprays employs spherical particles for the liquid phase. This was
because the initial research effort was formulated in terms of
spherical particles. However, as has been recently shown in ref-
erence 4, the air-shear breakup of modified fuels results in
stringlike and membranous particles, at least during the initial
stages of disintegration. At the moment is is not clear whether
or not these particles eventually breakup into droplets during a
crash as they move downstream from the aircraft, where the air
shear diminishes to zero. Therefore, the usefulness of a spray
burning velocity model that employs spherical particles becomes
questionable during the initial stages of disintegration, but may
still remain useful during the lifetime of the spray downstream
from the aircraft. For the present work the fuel particles were
modeled using an equivalent spray of spherical particles in order
to carry out calculations using the experimental results of ref-
erence 4.

EXPERIMENTAL WORK

MEASUREMENT OF THE DROPLET SIZE DISTRIBUTION IN SPRAYS.

Previous work on spray combustion (references 1, 2, 5, 6) has in-
dicated a strong influence of air-fuel ratio and droplet size on
calculated or measured burning velocities in a liquid fuel spray.
Although it is possible to obtain mean air-fuel ratios in experi-
mental test apparatus by measuring the average flow rates of fuel
and air through the test section, it is not easy to measure the
local mixture strength. Several attempts (references 2, 7, 8) have
been made to date to measure the droplet sizes in a polydisperse
spray using direct photography. Resolving small droplets on photo-
graphic film requires a high magnification, and as a result only a
small area of spray can be photographed at a time. Consequently,
the chance of recording the largest droplets, which may have a
droplet to droplet distance that is larger than the major dimension
of the area photographed, is relatively small, unless a very large
number of photographs are examined. In addition, it is difficult
to estimate which droplets are in and which are out of focus, and
the calculation of the air-fuel ratio from direct spray photographs
is questionable.

Compared to direct photography, a holographic technique of particle
size measurement (references 9, 10) offers the advantage of a large
depth of field compared to droplet size. This allows a large
spray volume to be recorded on one hologram, and later recon-
structed for detailed analysis. A hologram thus offers the

2

opportunity to calculate the instanstaneous air-fuel ratio of a large spray volume or of small parts of the volume recorded on the same hologram.

The following sections describe the work on the measurement of the droplet size distribution in kerosene-air sprays using a Fraunhofer (far field) holographic technique (reference 9). The spray generator was designed for the measurement of the burning velocity in sprays for which the local average velocity and the mean air-fuel ratio at the test section were independently measured. The mean air-fuel ratio could, therefore, be compared with the air-fuel ratio obtained from the measurement of the droplet size distribution. Preliminary results using the experimental apparatus described below were presented in reference 11. The following sections are an extension of the previous work and include the final results of the experiments.

EXPERIMENTAL APPARATUS.

The experimental apparatus consisted of three parts: (a) the spray generator, (b) the holocamera, and c) the reconstruction apparatus.

SPRAY GENERATOR. The spray generator was similar to the one used in a previous study (reference 2) with the liquid and air inlets redesigned for reducing the turbulence at the test section. Figure 1 is a schematic diagram of the spray generator. It consisted of three vertical sections with successively decreasing diameters in the flow direction connected with converging nozzles for smoothing out disturbances in the flow field. The last tube, with the smallest diameter, was 41 cm long and had a 19.5 mm ID. The overall height of the spray generator was 75 cm and was a compromise between the requirement for a low turbulence flow at the test section and sufficient aerodynamic drag for suspending the droplets. A 1 mm OD acetylene gas burner at the exit was used for pilot ignition of the spray which discharged vertically upwards into the ambient atmosphere. The primary air supply was metered using a rotometer, and a second rotometer was used for measuring the air supply to an ultrasonic atomizing nozzle operating at 35,000 cps. A water bath heat exchanger was used to increase the atomizing and primary air temperatures so that the air temperature at the 19.5 mm ID tube exit could be set to a maximum of 38°C. This enabled tests at elevated air temperature with the fuel inlet at a room temperature of 21°C. The fuel was supplied to the nozzle through a variable flow rate rotary pump, and the air-fuel ratio, as well as the droplet size distribution, were set by adjusting the pump exit pressure, and the primary and atomizing air flow rates. The average air-fuel ratio was calculated from rotometer readings, and by weighing the mixture collected at the tube exit using a plastic bag. The kerosene and air flow rates could be independently adjusted for obtaining a range of atomization and of air-fuel ratios
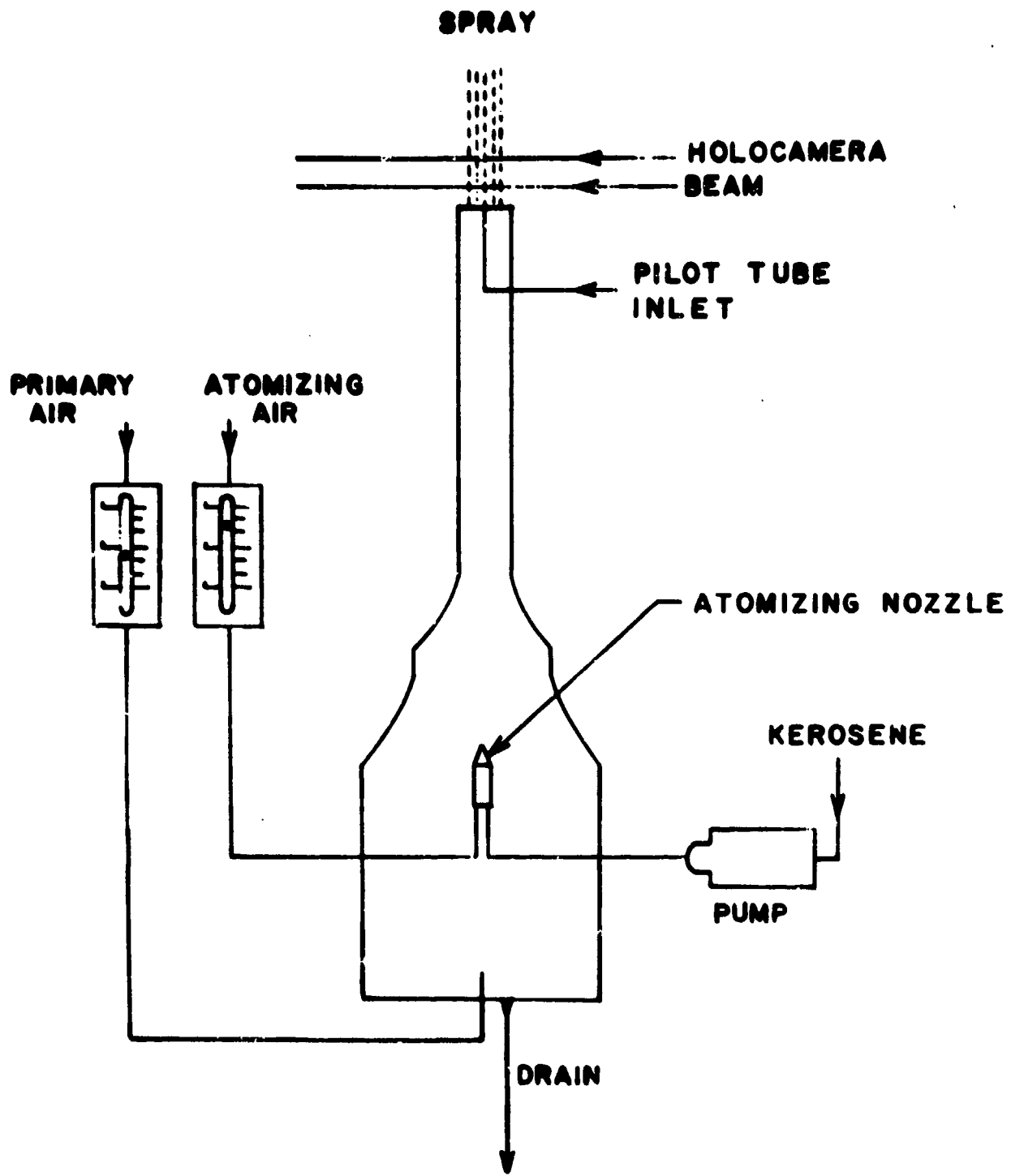
3

SPRAY

HOLOCAMERA
BEAM

PILOT TUBE
INLET

PRIMARY
AIR

ATOMIZING
AIR

ATOMIZING NOZZLE

KEROSENE

PUMP

DRAIN

FIGURE 1.   SCHEMATIC DIAGRAM OF THE SPRAY GENERATOR

4

at constant fuel and air supply flow rates. Figure 2 shows the distribution along the tube radius of mean velocity and rms velocity fluctuations measured with hot wire anemometry. The flow Reynolds number was 1950 based on the tube diameter, and the rms fluctuations were due to the jet instability associated with the air flow through the atomizing nozzle.

HOLOCAMERA. The holographic recording system used is shown schematically in Figure 3. It consisted of a holographic quality Q-switched ruby laser that produced a light pulse of 20 manoseconds duration and 1 mm in diameter. The ruby laser was aligned by a 2mw helium-neon laser. The output energy of the light was reduced by using only the light of the front surface reflection from an optical flat. The front surface reflection from the optical flat was expanded to a parallel beam of 40 mm diameter by a Galilean telescope. This light beam traversed the spray and was diffracted by the particles within the spray. Since the spray diameter was approximately 20 mm each hologram reproduced the whole spray width. A pair of lenses of 250 mm focal length were positioned behind the spray in order to reimage the spray at a one to one magnification (reference 12). The film could now be placed as close to the image of the spray as was necessary for the desired depth of field and resolution. The film used was Agfa 10E75AH in 4 x 5 inch glass plate format.

The recording distance, z_1 (shown in Figure 3), must be chosen carefully to match the range of droplet sizes being recorded. The in-line holographic technique requires that the wavefront be recorded in the "far field" of the droplet. Thompson et al (reference 9) have shown experimentally that the hologram should be between 1 and 50 far field numbers ($\lambda z_1/d^2$) from the droplet being recorded, i.e., $d^2/\lambda < z_1 < 50d^2/\lambda$, where λ is the wavelength of light and d is the diameter of the spherical droplet. On either side of this limit the reconstructed droplet image quality deteriorates rapidly. This permissible range of recording distances is illustrated in Figure 4 for far field numbers between 1 and 60. The vertical distance between the two slanted lines in Figure 4 represents the permissible range of z_1 for a droplet of the diameter marked on the abscissa. This vertical distance is essentially the depth of field for droplets of that diameter. However, in recording the sprays it is more convenient to use Figure 4 to estimate the range of droplet diameters that can be recorded in a plane a distance z_1 from the holographic plate. For example, at a plane that is 10 mm from the hologram all droplets in the range from 10.7 μm to 83 μm can be properly recorded and reconstructed. Figure 5 shows a photograph of an unreconstructed hologram magnified 4.7 times.

The number of droplets in the recording volume also affects the quality of the reconstructed image. If the spray is made up of too many droplets, insufficient undiffracted light reaches the holographic plate to provide the necessary reference wavefront.
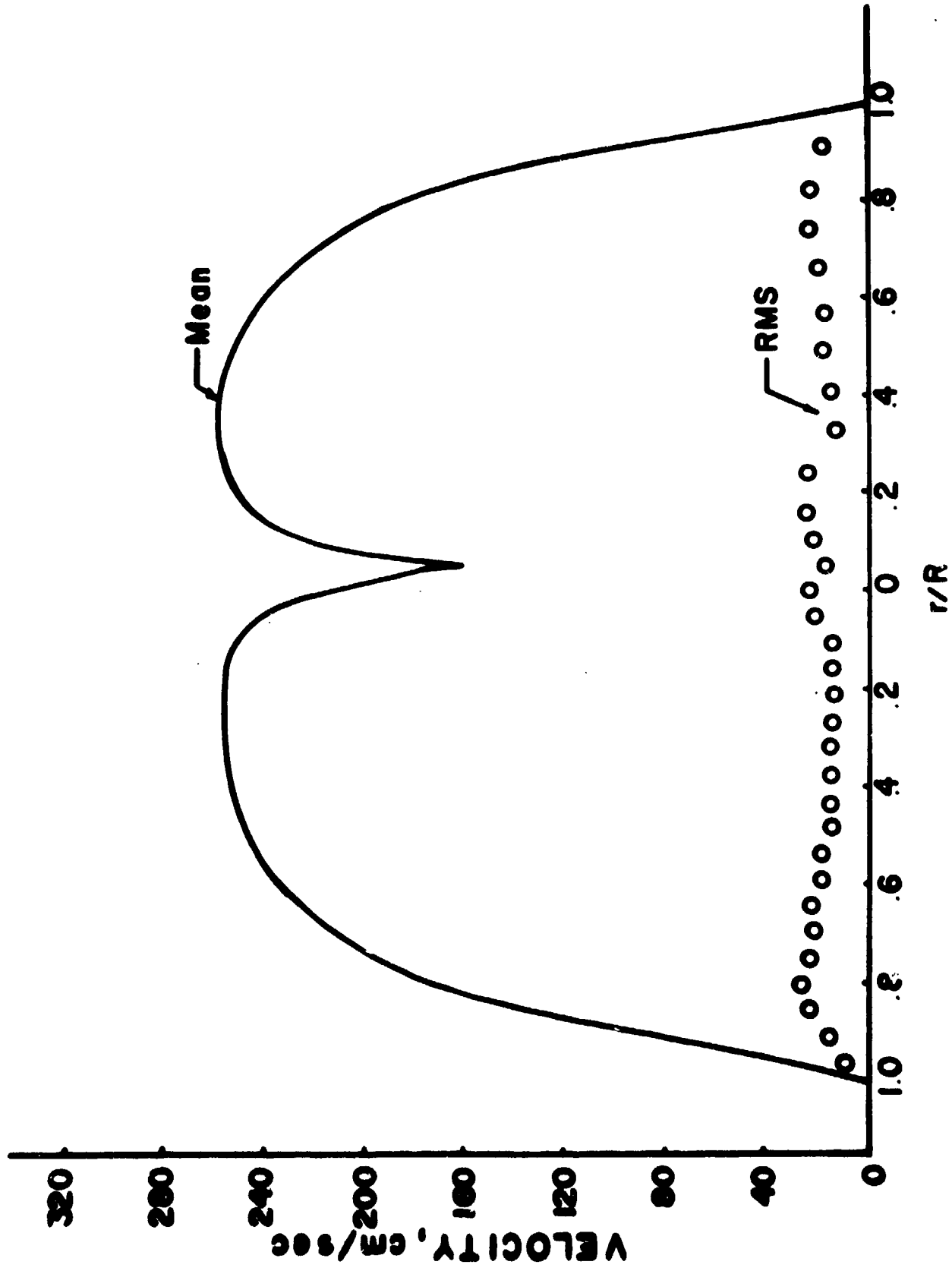
5

FIGURE 2. MEAN AIR VELOCITY AND RMS VELOCITY FLUCTUATIONS
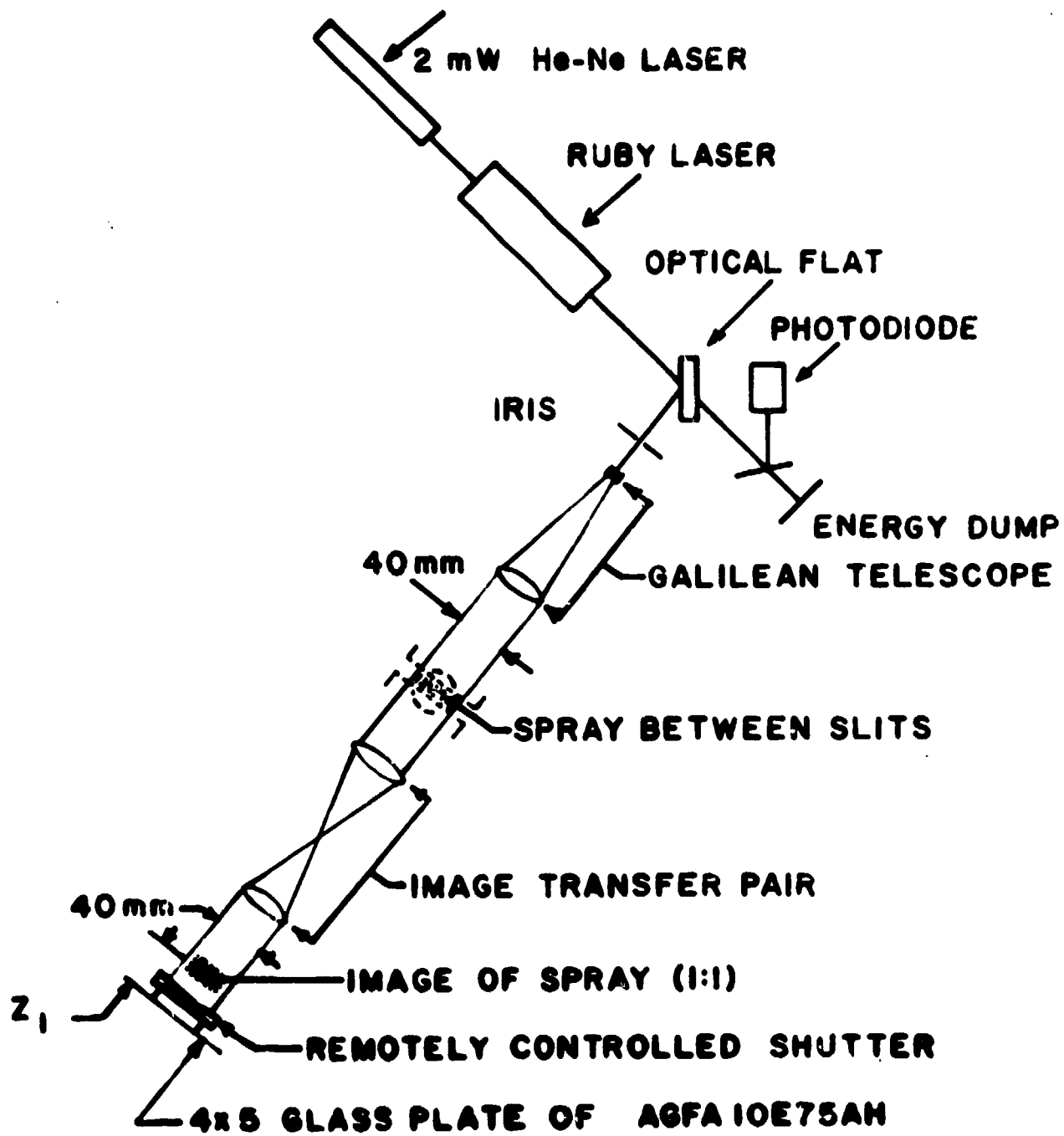AT THE TUBE EXIT

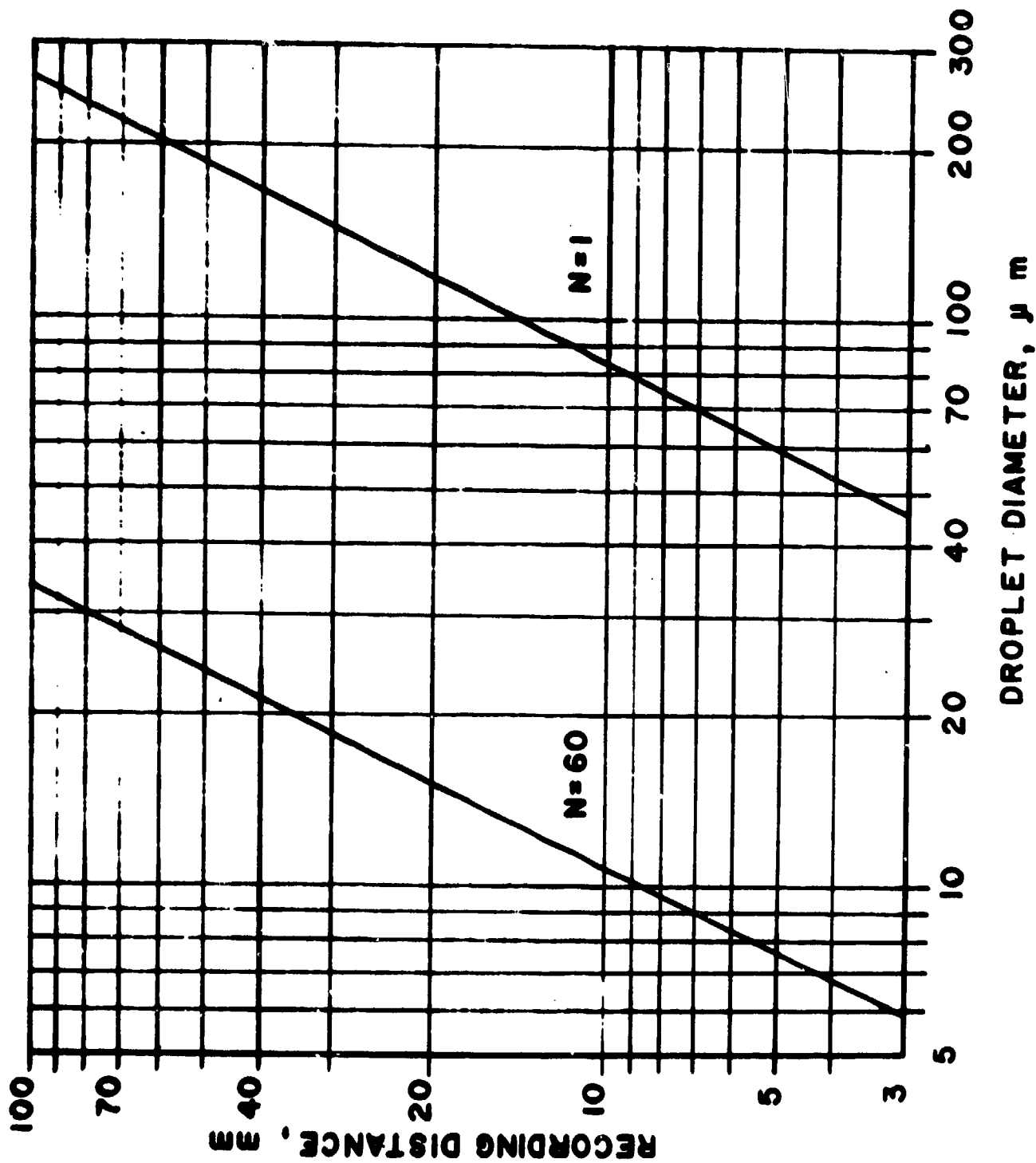FIGURE 3. SCHEMATIC DIAGRAM OF THE HOLOCAMERA

FIGURE 4. DROPLET DIAMETER VS. RECORDING DISTANCE FOR FAR FIELD IN-LINE HOLOGRAPHY

8

FIGURE 5. ENLARGED HOLOGRAM OF THE COARSE SPRAY. NO SLIT.

Ideally there should be no overlap at the holographic plate between the diffracted light from two adjacent droplets. Then the resolution of the system depends on the resolution of the film (reference 9), the resolution of the imaging lenses on Figure 3, as well as the resolution of the optics in the reconstruction apparatus. For our system this limit of resolution is about 4 μm. As the number of droplets increases, the diffracted light from adjacent droplets starts to overlap at the holographic plate and less undiffracted background illumination reaches the film. The resolution of small droplets is greatly affected by this condition but larger droplets (within the permissible range size) only become less sharp on the TV monitor. In effect the presence of many droplets in front of the holographic plate increases the size of the smallest resolvable droplet and blurs the reconstructed images of the larger droplets.

USE OF HOLOCAMERA IN DAYLIGHT. A feasibility study was carried out to see if the holocamera can be used to record droplet size distributions in full daylight. A narrow band filter, 50 mm in diameter, was installed inside the remotely controlled shutter (Figure 3) just in front of the recording film. The filter had a 70% transmission at the ruby laser wavelength of 6943 Angstroms and a band width of 100 A^{o}. The filter was very effective in blocking out undesired light from the brightly lit room and the ignited spray. However, the holograms produced with this filter in place reconstructed very poorly. The filter was made from a number of thin glass slides, sandwiched into a single unit. When the highly coherent laser light passed the filter, it produced many internal reflections from the glass interfaces and thus caused extensive interference patterns on the film. These strong interference patterns could be considered as noise that is superimposed on the Fraunhofer diffraction patterns caused by the spray droplets. As a result, the holograms taken through this filter reconstructed very poorly, and the use of this filter was discontinued.

The interference patterns might be eliminated if the filter were constructed from a single optical flat that has a multilayered thin film deposit on the front and an antireflection coating on the back side to prevent internal reflections within the glass. A filter of this construction was not obtained because a simpler solution was found by proper masking at the holocamera.

The majority of the stray light impinging upon the photographic film comes through the shutter at an oblique angle. This stray light from the room was blocked off with a bellowed tube extending from the shutter to the first lens of the image transfer pair (Figure 3). With this mask in place only the light that passed through the image transfer lenses reached the film. Experiments showed that the film was just faintly exposed when the shutter was left open for 30 seconds in a room in which the illumination was measured

10

to be 100 foot candles. Full sunlight gives an illumination of about 10,000 foot candles. Thus it seems that on a sunny day a comparable faint exposure due to stray light would be obtained with a shutter opening time of about .3 seconds (100/10000 x 30). In the present equipment the remotely controlled shutter was synchronized with the ruby laser to open for 1/3 second during which time the laser was fired. Since the 1/3 second shutter opening is approximately the same as the estimated 0.3 seconds required to record stray light in bright daylight, it is concluded that the present holo-camera without further modifications can be used to make high resolution holograms of sprays under outdoor lighting conditions.

RECONSTRUCTION APPARATUS. The reconstruction optical system is shown in Figure 6. A 5 mW helium-neon laser beam was expanded to a parallel beam of 50 mm by an expanding telescope. The 4 x 5 glass plate hologram was positioned on a precision x-y-z table and placed in the parallel light beam. A real image of the spray was thus reconstructed a distance z_2 behind the hologram where $z_2 = (\lambda_1/\lambda_2)z_1$, λ_1 and λ_2 are the wavelengths of the recording and reconstructing light, respectively. The size of the profile image of all particles within the reconstructed volume is the same as in the real spray since no scale magnification occurs in the lateral direction. However, the reconstructed spray volume is stretched in the longitudinal direction by a ratio of wavelengths of the recording light to the reconstructing light, i.e. a scale factor of (λ_1/λ_2).

The particles in the reconstructed spray were re-imaged by a simple lens on the vidicon tube of a TV camera and displayed on a TV monitor. The overall magnification was adjusted to 400X. In this way the view on the TV monitor represented a 1.0 mm x 0.89 mm lateral cross-section of the spray. The depth of field was essentially the depth of field permitted by the simple imaging lens. Because this lens was being used to greatly magnify the reconstructed spray particle, the depth of field was very shallow. A droplet was brought into focus on the monitor screen by moving the traversing table with the hologram on it along the direction of the light beam. This longitudinal motion of the hologram resulted in the whole reconstructed volume being moved towards or away from the imaging lens that was kept fixed in position. Since the plane of focus for the lens was a constant distance in front of the lens, this longitudinal motion of the hologram brought different lateral planes within the reconstructed volume into the plane of focus of the lens, and showed 1 x 0.89 mm sections of these lateral planes in sharp focus on the monitor screen. The longitudinal traversing direction of the x-y-z table was motorized to speed up this focusing procedure. The location of droplets within the reconstructed volume could be determined by the position of the x-y-z table, and their diameter was measured on the TV screen with a calibrated reticle.
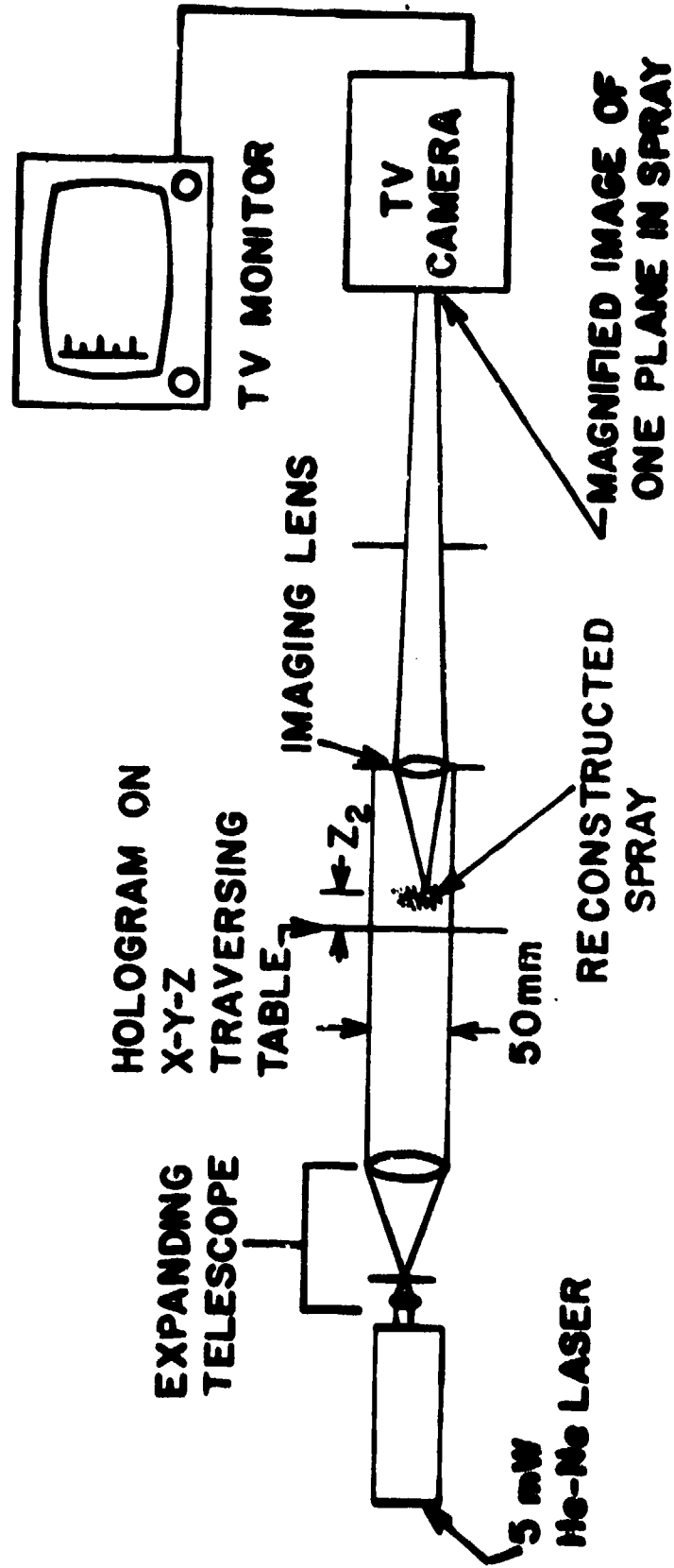
11

FIGURE 6. RECONSTRUCTION APPARATUS

EXPERIMENTAL PROCEDURE.

Holograms were recorded using sprays at several different mean air-fuel ratios and for two different upstream air temperatures. These are shown on Table 1 The gross particle size classification was obtained from visual observations of the spray, the Reynolds number, Re, is based on the 19.5 mm tube diameter, and the A/F denotes the mean air-fuel mass ratio calculated by collecting and weighing the fuel that leaves the tube during a measured time interval. To resolve the large number of small droplets present in the sprays, it was necessary to divert part of the spray away from the laser beam by using a 6 mm wide slit placed perpendicular to the flow direction as shown in Figure 3. For the slitted sprays tested the resolution was found to be 15 microns, however, only droplets above 20 microns were counted. Droplets smaller than 15 microns were also observed, but their diameter could not always be absolutely determined. During subsequent examination of the reconstructed holograms, it was found that large droplets (above 100 microns) were relatively scarce in the reconstructed volume directly above the slit where the counting was carried out. However, holograms without the slit revealed the presence of numerous droplets above the 100 micron range. It was concluded that the large shear gradients introduced across the 6 mm width of the slit resulted in a sideways deflection of the larger droplets away from the volume of spray under examination. It should be noted that the mean flow velocity in the region where the droplet counts were carried out was approximately 250 cm/sec, while the terminal velocity of droplets in the 100 to 300 micron range varied from approximately 20 cm/sec to 100 cm/sec. The concentration of small drops, which closely follow the flow shearlines, was not affected by the presence of the slit.

Information on the number of small and large sized droplets was therefore obtained by superimposing average counts obtained from different holograms of the same spray with and without the slit, respectively. Since it was difficult to resolve small droplets without the slit, only droplets with diameters larger than 100 microns were counted without the slit. With the slit present only droplets with diameters less than 100 microns were counted. The droplet counts were obtained using the same spacial volume for the slitted and unslitted cases. Figure 7 shows the position and size of the measuring cells which totaled 36 for each side of the tube. Each shaded rectangle represents a cell 1 mm by 0.89 mm x 6 mm deep. The droplet counts from the set of nine cells at each position along the tube diameter were added for obtaining the instantaneous droplet size distribution for each position. Total counts from stations 1 through 8 along the tube diameter were used for obtaining the average instantaneous droplet size distribution across the tube.

13

TABLE 1. EXPERIMENTAL CONDITIONS FOR THE SPRAYS TESTED

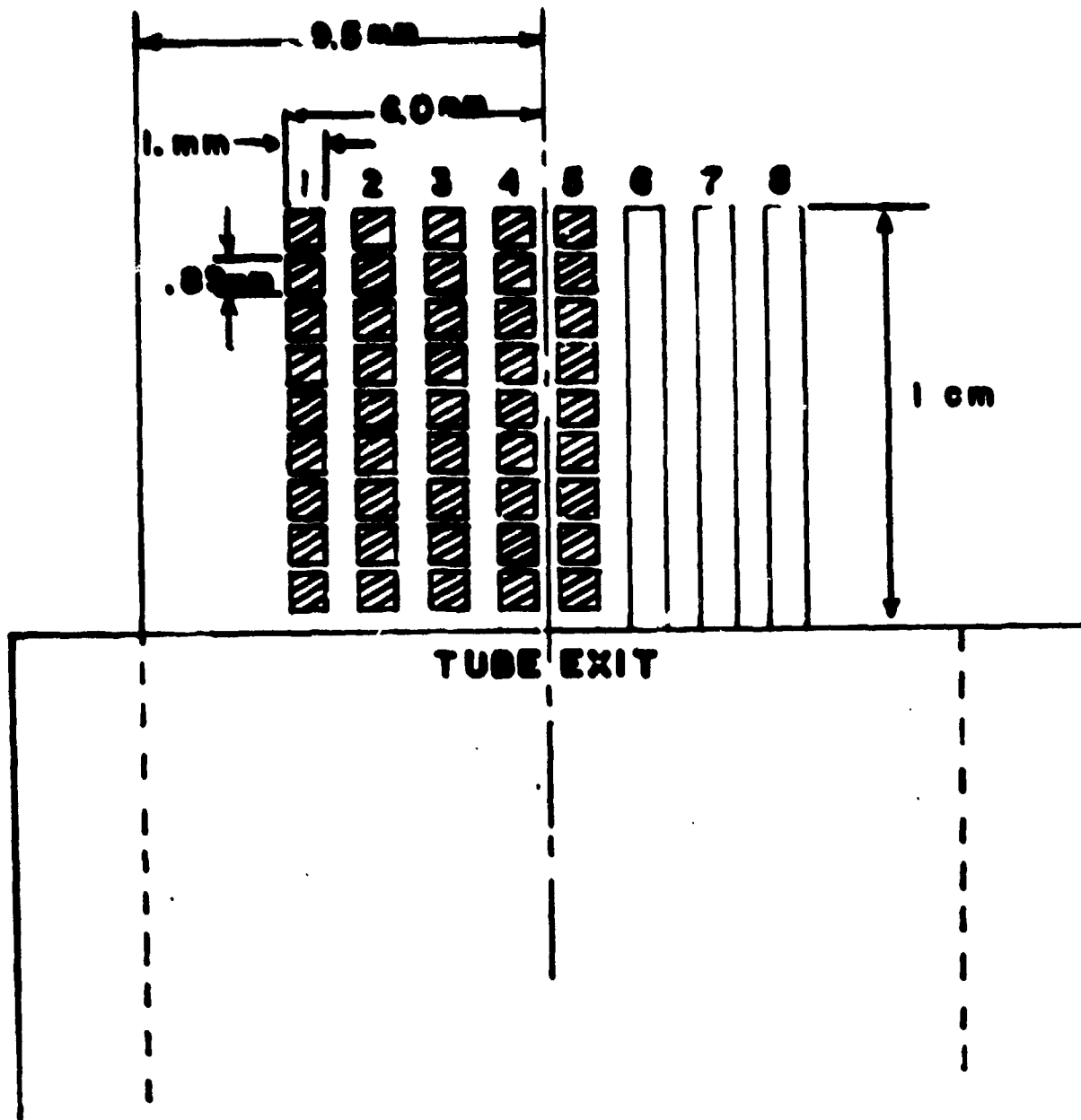| Spray	Gross Particle Size Classification	Upstream Air Temperature °C	Air Flow Rate m³/hr	Re	A/F
1	Fine	21	1.96	1,935	17
2	Intermediate	21	1.96	1,935	17
3	Coarse	21	1.96	1,935	17
4	Very Coarse	21	1.96	1,935	13.2
5	Heated Air	38	1.96	2,044	15

14

FIGURE 7. POSITION OF THE MEASURING CELLS AT THE TEST SECTION

15

RESULTS AND DISCUSSION

AVERAGE DISTRIBUTION OF DROPLET SIZE.

For each spray tested droplets from a total of four holograms were
counted, two with the slit, and two without the slit. Table 2 shows
the total counts within a 0.47 cm³ volume which is the volume of all
the measuring cells on Figure 7. (a) and (b) refer to counts ob-
tained from different holograms of the spray. On the same table D_m
denotes the diameter of the largest droplet seen anywhere inside the
reconstructed volume. D_m was used for the initial size distribution
plots as will be subsequently described. The very fine atomization
of the "Fine" spray (Table 1) prevented counting of all droplets in
that spray

The droplet size information recorded on a hologram is for an in-
stantaneous condition of the spray. Depending on the size of the
reconstructed volume that is scanned, it is possible to find large
differences in the number of droplets counted among different holo-
grams of the same spray if the droplet spacing is the same size as
the largest dimension of the scanned volume. This is particularly
true for the large droplets in the spray. A large number of holo-
grams is thus necessary for measuring time average droplet size
distributions in a small fixed volume. However, it should be ex-
pected that for droplets which are closely spaced, compared to the
size of the scanned volume, the fraction of each size counted will
remain relatively constant between holograms of the same spray.
As a result, for such droplets if the long time average droplet
size distribution within the spray volume is constant, then the
instantaneous size distribution should be a good approximation
of the average size distribution.

Sprays of interest in combustion problems contain droplets which
are too small to be optically resolved, and as a result, it is im-
possible to obtain directly from the droplet counts a numerical
distribution of all the sizes in the spray. On the other hand,
the volume of liquid in small droplet sizes is often a small pro-
portion of the total liquid volume. It is, therefore, possible
to construct a volume (or mass) distribution, provided that all
droplets of maximum size are included, since their volume is an
appreciable fraction of the total liquid volume.

The total number of droplets for each diameter size range in each
hologram was obtained by adding the counts in each cell for sta-
tions 1 to 8 (Figure 7). The spray volume under consideration
was, therefore, large, and there was a high probability of includ-
ing also the large sized droplets in the spray. Table 3 shows the
mass of liquid per unit volume calculated from the total sample of
droplets counted in each hologram. It shows that the mass of
liquid below 100 μm was relatively constant, while the mass of
liquid in the size range above 100 μm varied considerably between
holograms of the same spray. To arrive at a droplet size distribu-
tion function which reasonably approximates the distributions

16

TABLE 2a. DROPLETS COUNTED IN SPRAY 2 (INTERMEDIATE* SPRAY)

Diameter µm	Number of Droplets With Slit		Diameter µm	Number of Droplets Without Slit	
	(a)	(b)		(a)	(b)
20-25	128	138	100-105	10	3
25-30	103	101	105-110	4	2
30-35	72	72	110-115		
35-40	45	3d	115-120		
40-45	22	23	120-125		
45-50	23	19	125-130	1	1
50-55	8	12	130-135		1
55-60	9	4	135-140		3
60-65	4	6	140-145		
65-70	5	2	145-150	2	
70-75	2	5	150-155		
75-80	2	1	155-160	1	
80-85		3			
85-90					
90-95	1		175-180		1
95-100	1				
			185-190	1	
TOTALS	425	424		19	11

*Volume Scanned: 0.47 cm^3

D_m = 220 µm

17

TABLE 2b. DROPLETS COUNTED IN SPRAY 3 (COARSE SPRAY)

Diameter µm	Number of Droplets With Slit		Diameter µm	Number of Droplets Without Slit	
	(a)	(b)		(a)	(b)
20-25	122	147	100-105	2	3
25-30	110	119	105-110	4	2
30-35	55	74	110-115		
35-40	27	37	115-120	1	
40-45	11	19	120-125		2
45-50	19	11	125-130	2	2
50-55	8	3	130-135	1	
55-60	5	13	135-140		2
60-65	2	6			
65-70	8	6	165-170	2	1
70-75	5	5			
75-80	8	5	170-175		3
80-85	1	2	175-180	2	
85-90	1	3			
90-95	5	2			
95-100	3	2	245-250	1	
TOTALS	390	454		14	13

Volume Scanned: 0.47 cm^3

$D_m = 247$ µm

18

TABLE 2c. DROPLETS COUNTED IN SPRAY 4 (VERY COARSE SPRAY)

Diameter µm	Number of Droplets With Slit		Diameter µm	Number of Droplets Without Slit	
	(a)	(b)		(a)	(b)
20-25	134	130	100-105	4	4
25-30	63	74	105-110	1	2
30-35	28	39	110-115	2	
35-40	32	38	115-120	3	
40-45	21	17	120-125	1	2
45-50	14	18	125-130	1	1
50-55	8	14	135-140	1	1
55-60	15	19	140-145	1	
60-65	12	9	145-150	3	1
65-70	6	7	155-160	1	2
70-75	2	6	160-165	1	0
75-80	3	4	170-175	1	1
80-85	4	2	175-180	1	2
85-90	4	3	180-185	1	
90-95	3	2	185-190		1
95-100	6	1	190-195	1	
			200-205		1
			205-210		1
			215-220	2	
			225-230	1	
			230-235	1	
			250-255	1	
			285-290	1	1
			300-305	1	
			310-315		1
			315-320	1	
			325-330		1
			365-370	1	
			390-395	1	
TOTALS	355	383		33	22

Volume Scanned: 47 cm³
D_m = 382 µm

19

TABLE 2d.   DROPLETS COUNTED IN THE HEATED AIR SPRAY

Diameter µm	Number of Droplets With Slit		Diameter µm	Number of Droplets Without Slit	
	(a)	(b)		(a)	(b)
20–25	193	182	100–105	0	2
25–30	92	71	105–110	2	0
30–35	41	41	115–120	1	3
35–40	29	26	125–130	0	1
40–45	18	14	130–135	0	1
45–50	11	10	135–140	0	1
50–55	8	7	145–150	1	0
55–60	5	6	155–160	0	2
60–65	5	2	185–190	0	1
65–70	2	3	190–195	1	0
70–75	2	2	235–240	0	1
75–80	3	6			
80–85	2	2			
85–90	0	1			
90–95	0	1			
95–100	1	2			
TOTALS	412	376		5	12

Volume Scanned: 0.47 cm³

D_m = 247 µm

20

TABLE 3. LIQUID VOLUME CALCULATED FROM THE
DROPLET COUNTS OF EACH HOLOGRAM

Spray		Liquid Volume for $D_1 < 100$ μm cm^3	Liquid Volume for $D_1 > 100$ μm cm^3
Fine*		--	--
Intermediate	a.	1.11×10^{-5}	1.81×10^{-5}
	b.	1.08×10^{-5}	1.23×10^{-5}
Coarse	a.	1.50×10^{-5}	2.66×10^{-5}
	b.	1.47×10^{-5}	1.49×10^{-5}
Very Coarse	a.	1.68×10^{-5}	9.85×10^{-5}
	b.	1.54×10^{-5}	14.87×10^{-5}
Heated	a.	0.757×10^{-5}	0.757×10^{-5}
	b.	1.05×10^{-5}	1.97×10^{-5}

*Very fine atomization prevented accurate counting.

obtained from the holograms it was therefore necessary to use the average droplet counts for each size range, calculated for the different holograms of each spray. In addition, the droplet counts were grouped in size ranges which increased by $\sqrt{2}$, so that the liquid volume in each size range could be plotted using equal spacial intervals on a logarithmic plot. Table 4 shows the averaged droplet counts in each size range beginning with 20 μm diameter droplets. On the same table, Δ(volume) is the mean liquid volume calculated from the droplet counts in Table 2 using the relationship

$$\Delta(\text{volume}) = \frac{\pi}{6} \Sigma N_1 D_1^3 \qquad (1)$$

where N_1 is the mean number of droplets in each 5 μm diameter range of Table 2.

Previous work (reference 13) has shown that droplet size distribution can best be approximated using an Upper-Limit Log-Normal size distribution function. This distribution function is given by the following equation:

$$\frac{dv}{dy} = \frac{\delta}{\sqrt{\pi}} e^{-y^2 \delta^2} \qquad (2)$$

where v is the fraction of spray volume contained in droplet sizes below a diameter D, and

$$y = \ln\left(\frac{aD}{D_m - D}\right) \qquad (3)$$

δ and a are constants to be determined experimentally. D_m is a third constant which corresponds to the maximum droplet diameter in the spray. Therefore, fitting an Upper Limit Distribution function to a set of data involves fixing the values of the three constants, a, δ and D_m, as well as the knowledge of the total liquid volume, V_T, of the sample. Determination of the total spray volume is not a straight forward process if (a) there is a large number of droplets which are too small to be resolved by the experimental apparatus, and (b) the droplet sample is incomplete, resulting in droplet counts which do not vary smoothly among adjacent size ranges.

The following procedure was adopted for the estimation of the spray volume V_T as well as of a, δ and D_m:

(1) The experimental data on Table 4 for each spray was plotted on a logarithmic plot as a histogram of Δ(volume)/Δ(lnD) versus 100 D/D_m. D_m was the maximum droplet diameter observed at the

22

TABLE 4a. DROPLET COUNTS IN SIZE RANGES
WHICH ARE MULTIPLES OF $\sqrt{2}$

INTERMEDIATE SPRAY

Size Range μm	Mean Number of Droplets	Δ(volume) cm^3
20.00 - 28.28	202	1.52×10^{-6}
28.28 - 40.00	149	2.82
40.00 - 56.57	58.8	3.06
56.57 - 80.00	15.6	2.72
80.00 - 113.14	12.5	6.77
113.14 - 160.00	4.5	6.42
160.00 - 226.27	1.15	4.01
226.27 - 320.00	--	--
320.00 - 452.55	--	--

TABLE 4b. DROPLET COUNTS IN SIZE RANGES
WHICH ARE MULTIPLES OF $\sqrt{2}$

COARSE SPRAY

Size Range µm	Mean Number of Droplets	Δ(volume) cm³
20.00 - 28.28	210	1.61×10^{-1}
28.28 - 40.00	137	2.46
40.00 - 56.57	317	2.12
56.57 - 80.00	35.3	4.81
80.00 - 113.14	15.0	7.15
113.14 - 160.00	5	5.51
160.00 - 226.27	2.5	5.26
226.27 - 320.00	0.5	3.96
320.00 - 452.25	--	--

24

TABLE 4c. DROPLET COUNTS IN SIZE RANGES
WHICH ARE MULTIPLES OF $\sqrt{2}$

VERY COARSE SPRAY

Size Ranges μm	Mean Number of Droplets	Δ(volume) cm^3
?0.00 - 28.28	177	1.28×10^{-6}
28.28 - 40.00	92	1.83
40.00 - 56.57	51	3.03
56.57 - 80.00	36	5.20
80.00 - 113.14	19	8.54
1∴.1⁴ - 160.00	10	15.55
).00 - 226.27	7	31.51
226.27 - 320.00	4.25	46.67
320.00 - 452.25	1.50	36.90

TABLE 4d. DROPLET COUNTS IN SIZE RANGES
WHICH ARE MULTIPLES OF $\sqrt{2}$

HEATED COARSE SPRAY

Size Ranges μm	Mean Number of Droplets	Δ(volume) cm^3
20.00 - 28.28	241	1.70×10^{-6}
28.28 - 40.00	97	1.80
40.00 - 56.57	36	1.97
56.57 - 80.00	16	2.72
80.00 - 113.14	10	2.91
113.14 - 160.00	4	6.42
160.00 - 226.27	1.0	3.59
226.27 - 320.00	.5	2.40
320.00 - 452.25	--	--

tube exit, Δ(volume) was obtained from Table 4, and $\Delta(\ln D)=0.346$.

(ii) A smooth curve approximating the shape of an upper-limit type curve was then drawn to fit the experimental data. Figure 8 shows the results of steps (i) and (ii) for the intermediate spray.

(iii) It was assumed that the curve drawn on Figure 8 is a reasonable approximation of the data that would have been obtained if the droplets counted were a complete sample. As a result, integrating the area under this curve should yield an estimate of the total liquid volume present within the spatial volume scanned in the holograms. For sprays where the size range with the maximum liquid volume is within the resolution of the experimental apparatus, the calculated value of V_T is relatively insensitive to slight changes in the position of the smooth curve drawn in (ii). For the distributions obtained in the present study the lowest droplet diameter was assumed to be 5 μm. Droplets smaller than 5 μm had a negligible effect on V_T.

(iv) From the intermediate values of the liquid volume computed in (iii), and using V_T, it was possible to construct a cumulative liquid volume distribution. Using the procedure suggested in reference 13, it was then possible to calculate a, δ, and D_m.

(v) The experimental data were then replotted using the calculated value of D_m. The corresponding upper limit curve was also plotted on the same graph to test agreement. Figure 9 shows the final results for the intermediate spray, and Figures 10-12 show the final distributions for the remaining sprays whose droplets were counted. In all cases the agreement was satisfactory.

Table 5 shows the spray maximum diameter, D_m, and the Sauter mean diameter, D_{32}, using the procedure outlined above. The experimentally determined D_m and D_{32} are also shown for comparison. It should be noted that the experimental value of D_{32} is always higher than that predicted by the upper-limit function, since the latter includes droplets which are too small to be resolved by the experimental apparatus. Since the spray sample does not necessarily include the maximum sized droplets, the largest droplets observed in each spray are smaller than the value of D_m in the upper-limit function.

AIR-FUEL RATIO MEASUREMENTS.

It is possible to calculate the air-fuel ratio using the information obtained from the holograms, together with the measured air flow rate through the apparatus. To accomplish this calculation it is necessary to (a) consider the slip velocity between the droplets and the gas, and (b) to account for the fuel that has evaporated inside the spray generator. The air-fuel ratio thus obtained can then be compared with that measured by collecting, over a fixed period of time, the mixture at the spray generator tube exit.

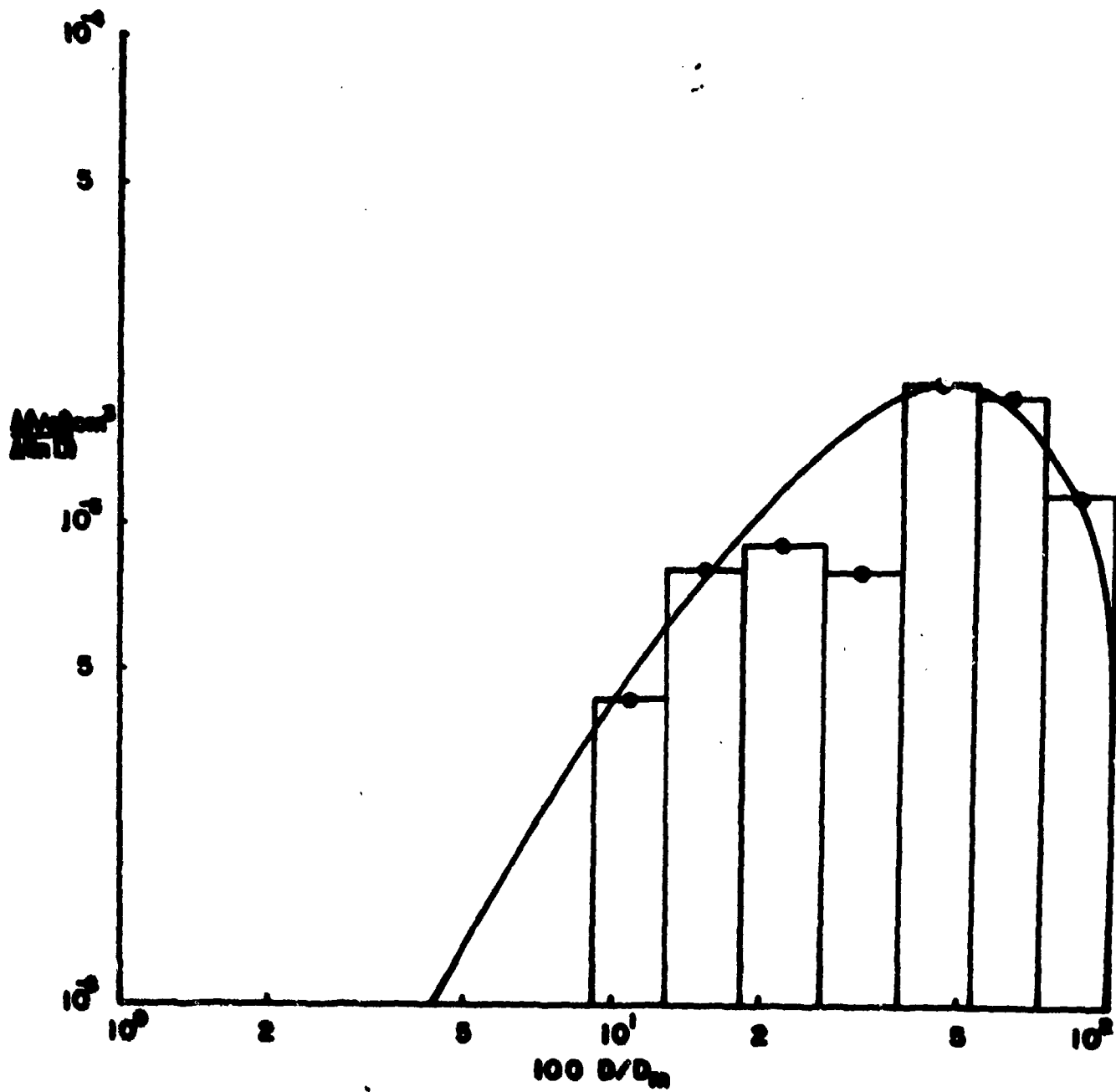The air-fuel ratio based on the liquid volume present is calculated

FIGURE 8. FIRST PLOT OF THE DROPLET SIZE DISTRIBUTION
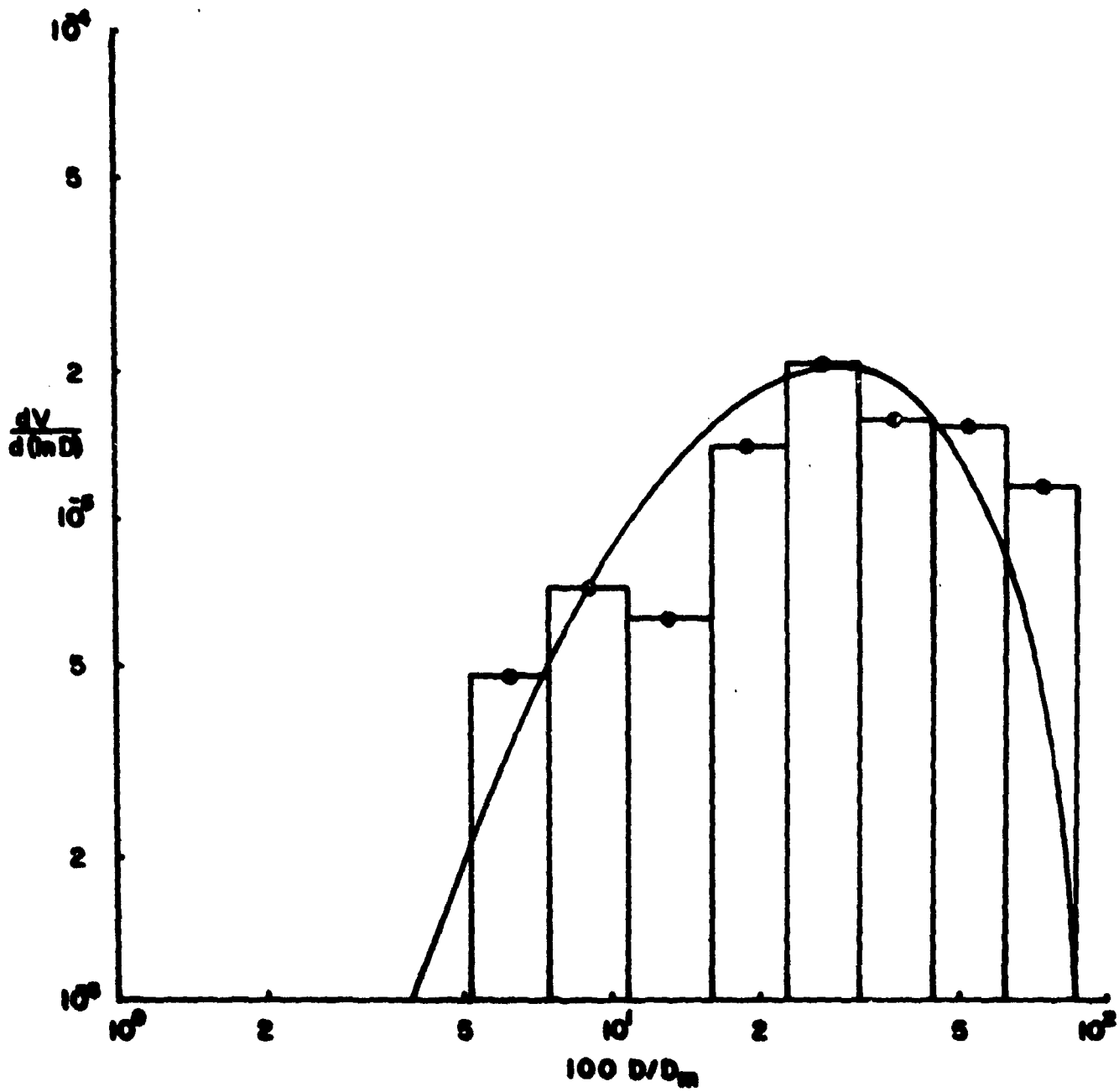FOR SPRAY 2

28

FIGURE 9.   FINAL PLOT OF THE DROPLET SIZE DISTRIBUTION
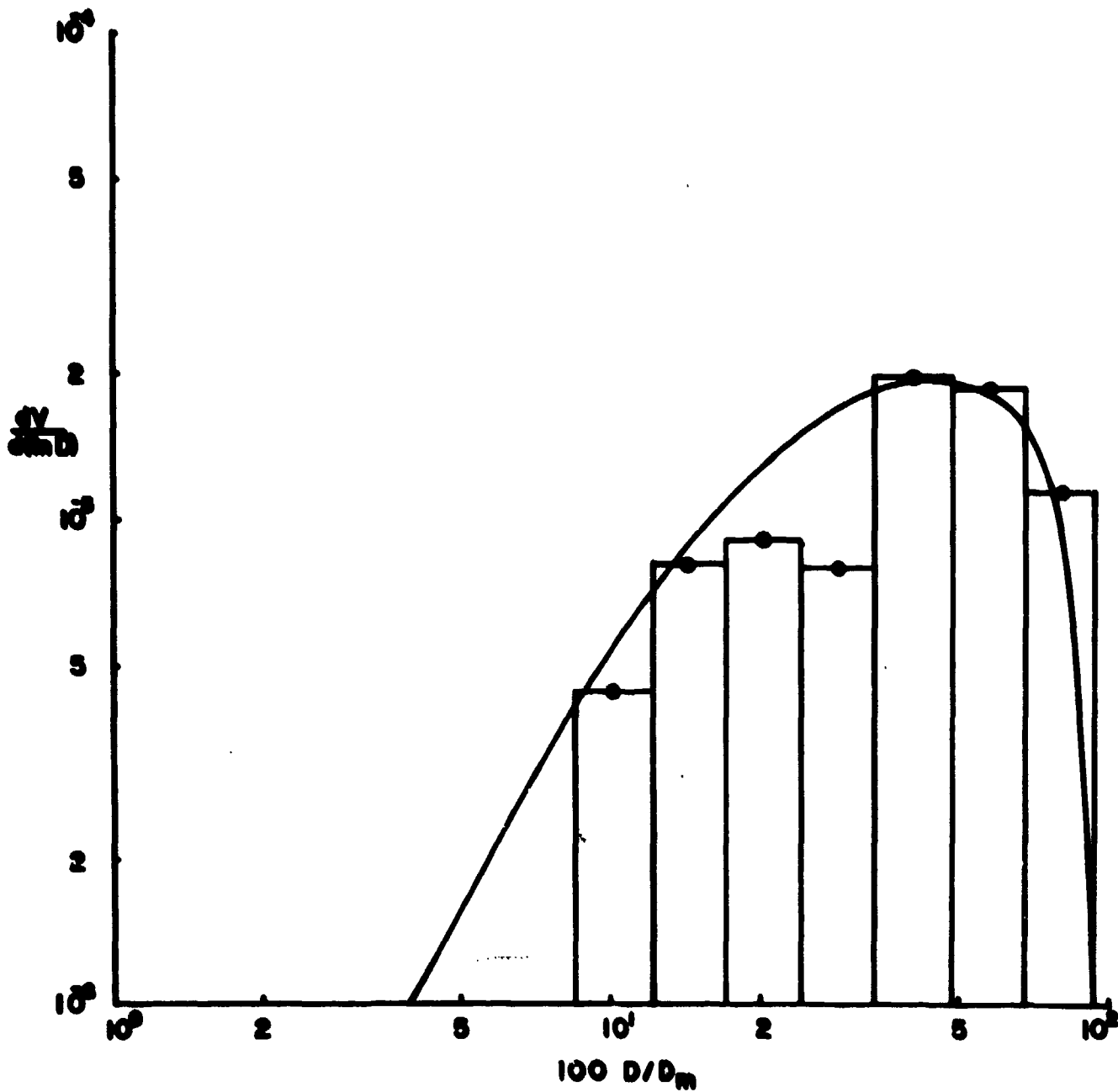FOR SPRAY 2

29

FIGURE 10. FINAL PLOT OF THE DROPLET SIZE DISTRIBUTION
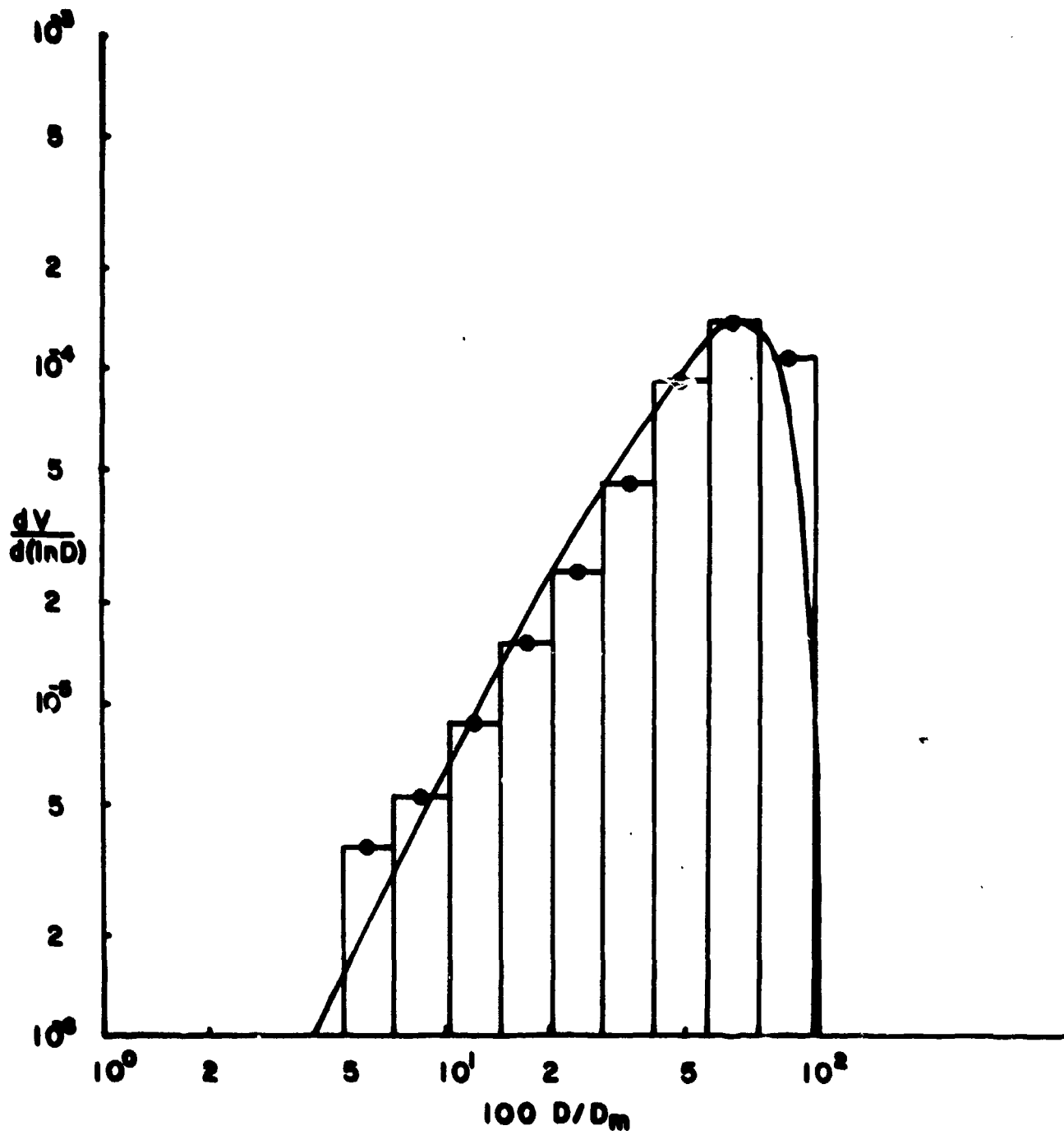FOR SPRAY 3

30

FIGURE 11. FINAL PLOT OF THE DROPLET SIZE DISTRIBUTION
FOR SPRAY 4

31
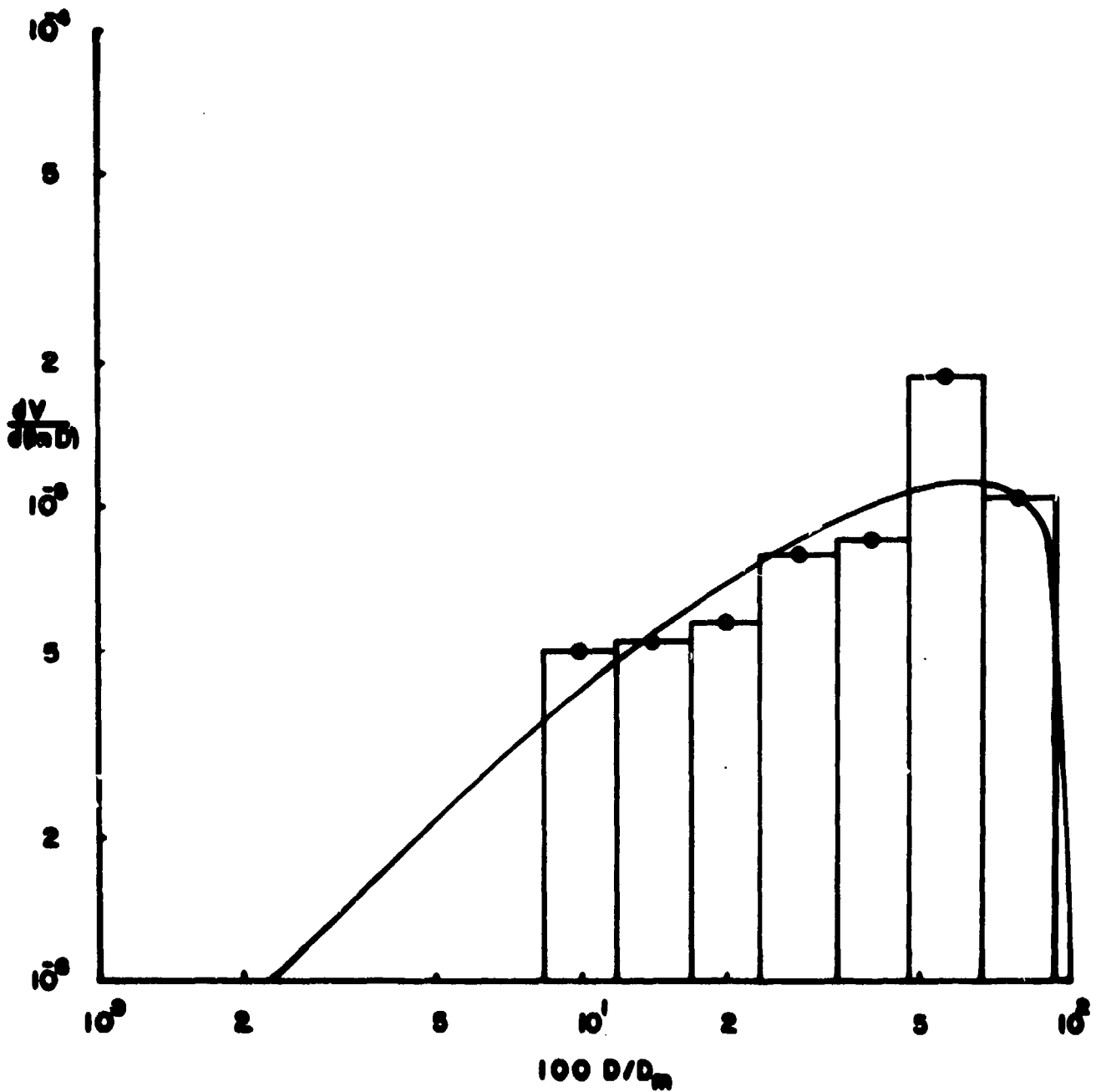
FIGURE 12. FINAL PLOT FOR THE DROPLET SIZE DISTRIBUTION FOR SPRAY 5

32

TABLE 5. EXPERIMENTAL AND CALCULATED MAXIMUM AND
MEAN DROPLET DIAMETERS OF THE SPRAYS TESTED

Spray	D_{32}, μm $\quad$ D_m, μm (Upper Limit Distribution)		D_{32}, μm $\quad$ D_m, μm (Data)	
Fine	--	--	--	--
Intermediate	50	236	69	220
Coarse	60	376	79	247
Very Coarse	140	392	147	382
Heated	36	308	63	240

using the following relationship:

$$(A/F)_{\ell} = \frac{\rho_a}{\rho_s} \tag{4}$$

$$\text{where } \rho_s = \frac{\rho_{\ell}}{V_s} \sum_1 V_{si} \left(1 - \frac{V_1}{V_a}\right) \tag{5}$$

ρ_a is the air density, ρ_{ℓ} is the liquid density, V_{si} is the liquid volume in the size range D_i, V_1 is the terminal velocity of droplets of size i, and V_a is the mean air velocity in the volume of scanned spray. From figure 2, V_1 was taken to be 250 cm/sec and V_1 was calculated from standard drag coefficient relations (reference 14). The spray volume V_{si} was obtained from the values corresponding to the solid line of Figure 8 for the intermediate spray, and from similar figures for the remaining sprays. V_s was the physical volume scanned for obtaining droplet counts.

The vaporization from the spray was estimated from the one-dimensional spray model described in reference 1 applied without chemical re-action and with constant gas temperature. This permitted the con-servation equations for the liquid, which are described in reference 1, to be integrated using a step by step method over the 75 cm of length of the spray generator. The initial fuel vapor concentration in the gas stream was assumed to be zero. The resulting concentration at the tube exit was used to estimate the amount of fuel evaporated. The sprays were assumed to be monodisperse with initial droplet diameter equal to the Sauter mean diameter calculated from the Upper Limit function. The initial liquid fuel concentration in the spray was calculated from the measured F/A for each spray. Table 6 shows the physical properties that were employed for the calculation. The boiling point of the fuel depended on the fraction of liquid evaporated according to expected distillation data for Jet A which is also shown on the same table.

Table 7 shows the air to fuel mass ratio $(A/F)_c$, calculated from the droplet counts and from the estimated fuel vapor content of the tube exit. The air to fuel ratio measured by weighing the mixture at the tube exit, (A/F), is also shown for comparison. $(F/A)_{\ell}$ and $(F/A)_V$ on Table 7 denote the measured and calculated liquid and vapor content of the sprays, respectively. The result-ing air-fuel ratios are in good agreement except for the very coarse spray, where because of the richness of the mixture and the very large droplets present it was difficult to accurately collect and weigh the suspension at the tube exit. The results also indicate the significant effect of elevated air temperature on the vaporization from the spray.

TABLE 6. PROPERTIES USED FOR ESTIMATING
VAPOR CONTENT OF THE SPRAYS TESTED

c_p = 0.24 cal/g°K

L = 61 cal/g fuel

k = 6 x 10^{-5} cal/sec cm°K

M_F = 170 g/mole

T_B = 460°K   10% evaporated
       467°K   20% evaporated
       488°K   50% evaporated
       524°K   90% evaporated

TABLE 7. ESTIMATED LIQUID AND VAPOR CONTENT
OF THE SPRAYS TESTED

Spray	$F/A)_\ell$	$F/A)_v$	$A/F)_c$	A/F
Fine	--	--	--	17
Intermediate	0.044	0.005	20.4	17
Coarse	0.049	0.003	19.2	17
Extra Coarse	0.14	negligible	7.1	13
Heated	0.035	0.025	16.7	15

LOCAL DISTRIBUTION OF DROPLET SIZES.

Examination of the raw data showed that, except for the region di-
rectly above the igniter tube, there was no preferential position in
the spray for counting the relatively few large droplets present.
To obtain an estimate of the uniformity of the sprays tested, it is
possible to assign a maximum permissible difference, within a given
level of significance, to cumulative number distributions from samples
of the spray obtained from the different small volumes of the same
spray. The absence of large droplets, which were few in number, will
not appreciably affect such cumulative number distributions plotted
on η vs. D coordinates where η is the fraction of droplets below
size D. The Kolomogorov-Smirnov (reference 15) test for a two-sample
statistic can be used for calculating a maximum permissible difference,
and the results are shown on Figure 13 for the intermediate spray. The

relationship: $\pm 1.36 \ [N_1+N_2/N_1 N_2]^{\frac{1}{2}}$ gives the maximum permissible dif-

ference between two cumulative number distribution of two samples at
the 0.05 level of significance. N_1 and N_2 are the total number of
droplets counted in each sample. The number of droplets, N, at
various stations across the test section is shown on Figure 13.
Using any two of these counts as N_1 and N_2 in the previous formula
results in at most ±0.1. This is the maximum permissible difference,
at the 0.05 level of significance between the mean cumulative dis-
tributions of any two spray samples indicated on Figure 13. The
envelope between the dotted lines shows the permissible difference
in graphical form. Since all the distributions are within this
envelope, it can be concluded that 95% of the time small sample
cumulative number distributions will have at most a 10% maximum dif-
ference from the corresponding mean distribution of the spray.
Similar plots can be drawn for the other sprays tested with equiva-
lent results. Thus, the spray appears to be spatially uniform, at
least with respect to the numerical distribution of the droplet
sizes.

MEASUREMENT OF BURNING VELOCITIES.

EXPERIMENTAL PROCEDURE. Measurements of burning velocities in neat
kerosene-air sprays were previously carried out under the present con-
tract and the results were reported in references 2 and 3. These meas-
urements employed sprays where the droplet size distribution was only
qualitatively known from direct photographs of the cold spray. The
upstream gas flow had a relatively high turbulence intensity of approxi-
mately 9% in the region of burning velocity measurement, and the
Reynolds number based on the spray diameter was 2700. In the previous
sections of this paper, sprays used for the holographic work were des-
cribed accurately in terms of droplet size distribution, and air-fuel
ratio. For these sprays the approach gas flow was at a turbulence in-
tensity of 5%, as shown on Figure 2, and the Reynolds number was 1950.
Burning velocity measurements were also carried out for these sprays.
The experimental results were then compared with predictions of the
spray model (references 1 and 3) using upstream boundary conditions
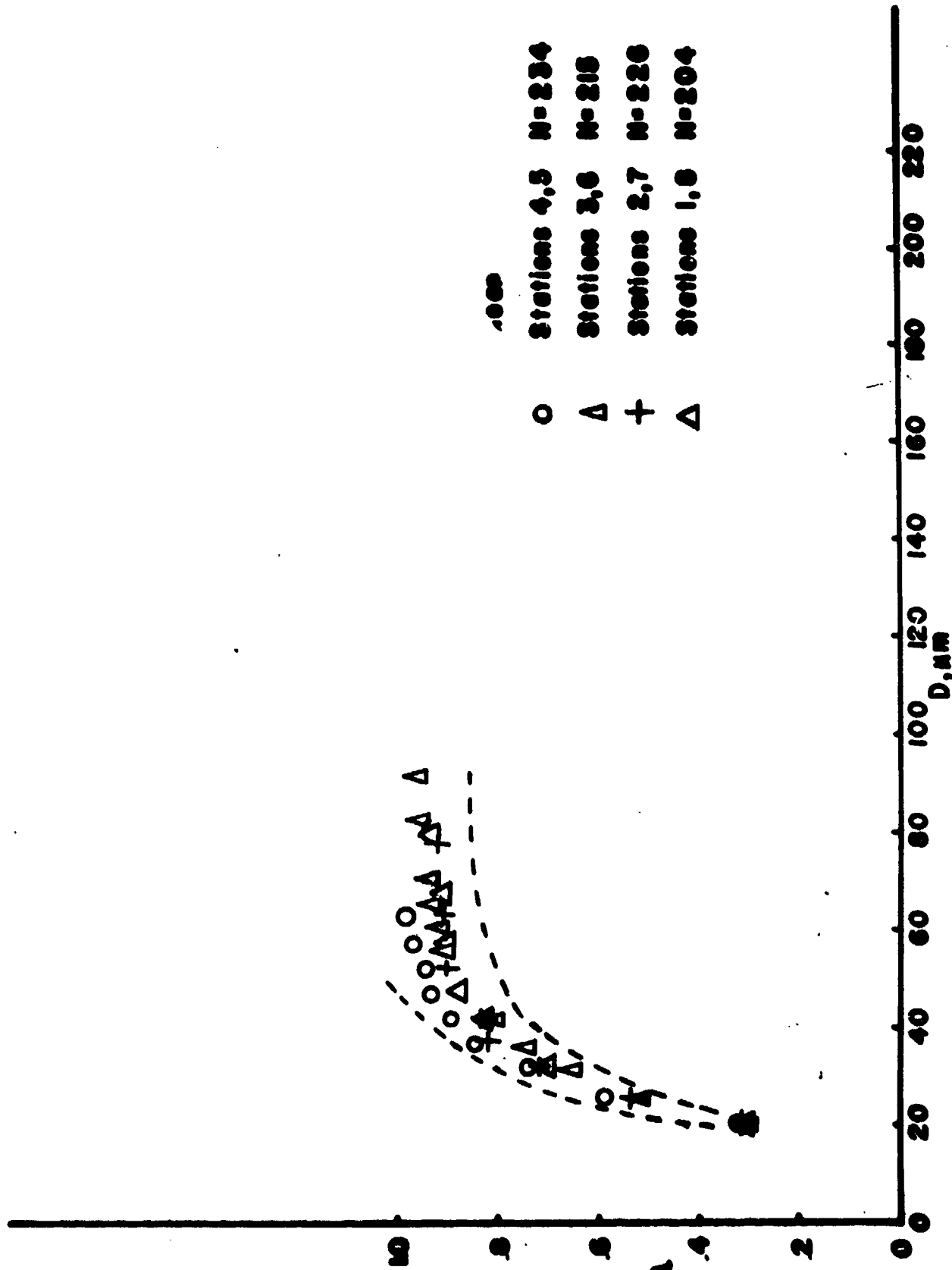equivalent to those employed during the experimental measurements.

37

FIGURE 13. CUMULATIVE MEASURED NUMBER DISTRIBUTIONS FOR VARIOUS SAMPLES OF THE INTERMEDIATE SPRAY 2

Attempts to measure burning velocities in modified fuels using
the present apparatus proved unsuccessful. This was because it
was not possible to entrain a sufficient number of large particles,
such as those present in a modified fuel suspension, and the re-
sulting flow at the tube exit was too lean to sustain a continuous
combustion wave.

RESULTS AND DISCUSSION. Table 8 shows the measured burning
velocities for the sprays tested, together with the calculated pre-
dictions using the previously developed spray model. To simulate
the turbulence level of the approach flow, the transport properties
of the gas were calculated using the eddy diffusivity model des-
cribed in reference 3. The turbulence intensity and turbulence
length scale used for the calculations are also indicated on
Table 8. The length scale was not measured experimentally, and
was assumed to be 0.5 cm, equal to one half of the tube radius.
The mixture physical properties were the same as those used for a
similar calculation in reference 3, and the sprays were represented
in terms of their Sauter Mean Diameter, D_{32}, calculated from the
Upper-Limit Log Normal distribution function (Table 5).

In addition to calculated values from reference 1, Table 8, also
shows calculated results using the following empirical relation
developed in reference 6 for kerosene-air sprays:

$$\text{Burning velocity} = \frac{6800}{D_{32}} \left(\frac{F}{A} - 0.012\right) (u') \ \frac{cm}{sec} \tag{6}$$

where u' is the rms velocity fluctuations in cm/sec and D_{32} is in
μm. The elevated upstream air temperature of spray 5, which re-
sulted in a considerable amount of vapor in the mixture prevented
comparison with equation (6), which was developed for sprays with
very little preignition vaporization. Lack of knowledge of D_{32} for
spray 1 prevented the calculation of the burning velocity in this
spray also.

The results of Table 8 show that both the model of reference 1
and equation (6) yield satisfactory agreement with experimental
data. However, equation (6) is not capable of predicting burning
velocities for very small droplet sizes, where there is appreciable
preignition vaporization.

BURNING VELOCITIES IN MODIFIED FUEL SPRAYS

Experimental work at the NAFEC five foot airflow facility
has resulted in photographs of fuel particles formed by air shear-
ing of modified fuels injected in an air stream with a nominal air
velocity of 110 knots. The results of this work are described in
reference 4. Based on the photographic evidence, an approximate

TABLE 8.   EXPERIMENTAL VS. CALCULATED BURNING
VELOCITIES OF NEAT JET A SPRAYS*

Spray	Burning Velocity, cm/sec.		
	Experimental	Calculated	
		Reference 1	Reference 6
1	64	–	–
2	77	70	67
3	64	56	54
4	65	45	69
5	105	85	–

*Calculated values were obtained as in reference 3 using a
turbulence length scale of 0.5 cm and a turbulence intensity
of 5%.

40

mean particle size and shape for three modified fuels was submitted by the investigators of reference 4 for calculations of burning velocities using the model of reference 1. The air shear disintegration of the modified fuels generates mostly thread-like and membranous particles. It was decided that, for the burning velocity calculations, the particles from each fuel would be characterized in terms of one mean cylindrical shaped particle with a mean diameter and a mean length. Ignoring the membranous particles was justified in terms of their apparently small liquid volume compared to the cylindrical particles. Determination of the mean sizes was carried out from photographs of the spray. Table 9 shows the measured particle sizes for the three fuels tested.

The model developed in reference 1 was for spherical particles only. In principle, adaptation of the model to cylindrical shaped particles involves the substitution of drag coefficient and evaporation rate relations for such particles in an air stream. Since such expressions were not available, it was decided to employ an equivalent monodisperse spherical particle spray for the burning velocity calculations.

A monodisperse spherical particle spray equivalent to a suspension of monodisperse cylindrical particles can be defined if it is assumed that the spheres and the cylindrical particles have the same diameter, the same density, and the same rate of decrease of diameter during evaporation. In addition, the equivalent spray should have the same total evaporation rate, the same total amount of fuel burned, and the same liquid particle heat-up rate as the cylindrical particle spray.

Assuming equal particle diameters, as well as equal rate of diameter decrease due to vaporization, the ratio of spherical to cylindrical spray vaporization is given by the following relationship:

$$\frac{\dot{m}_s}{\dot{m}_c} = \frac{n}{n_c} \frac{D}{\ell} \tag{7}$$

where ℓ is the length of the cylindrical particles, n_c is their number per unit volume, and D is the particle diameter. n_c can be calculated from the air-fuel ratio of the suspension. For the same liquid mass, the following relationship for the equivalent number of liquid droplets per unit volume, n, can be derived by equating the liquid mass in spherical and cylindrical particle sprays:

$$n = (\frac{\ell n_c}{D}) \frac{3}{2} \tag{8}$$

Substitution of equation (8) in (7) results in $(\dot{m}_s/\dot{m}_c) = 3/2$. As a result, the number of spherical droplets per unit volume that were employed was $2n/3$ where n is given by equation (8).

41

TABLE 9. MEAN CYLINDRICAL PARTICLE SIZE OF FUELS USED IN AIR SHEAR TESTS (REFERENCE 5)

Additive	Diameter μm	Length/Diameter
Neat Jet A	254	Spheres
0.2% AM-1	254	500
0.4% FM-4	762	50
0.7% XD 8132.01	2,540	50

To simulate the behavior of a cylindrical shaped particle spray, the evaporation rate of the spherical sprays, m_s, was, therefore, decreased by a factor of (3/2) during the calculations. This resulted in equivalent heat release rates during combustion, since the heat release rate is proportional to the liquid evaporation rate.

The heat balance for a cylindrical shaped fuel particle is given by the following equation:

$$\frac{dT}{dt} = \frac{4N_u k}{\rho_\ell c_{p_\ell} D^2} (T_\infty - T_s) + \frac{8L}{c_{p_\ell} D} \frac{dD}{dt} \tag{9}$$

where t is the time, $N_u = hD/k$ is the Nusselt number, h is the heat transfer coefficient, and c_{p_ℓ} is the liquid heat capacity. A similar relationship can be written for a spherical particle:

$$\frac{dT}{dt} = \frac{6N_u k}{c_{p_\ell} \rho_\ell D^2} (T_\infty - T_s) + \frac{12L}{c_{p_\ell} D} \frac{dD}{dt} \tag{10}$$

Using the previous assumptions, and assuming further that the Nusselt numbers are the same, the heat-up rate for a spherical particle (equation 10) becomes equivalent to that of a cylindrical particle (equation 9), if during the calculations the specific heat of the liquid, c_{p_ℓ}, is increased by 3/2.

Lack of knowledge of the orientation of the cylindrical particles in the air stream prevents making any assumptions regarding frictional drag, except that the equivalent spherical particles are governed by the drag relations discussed in reference 1.

It should also be noted that provided the air-fuel ratio and the particle diameter remain constant, there is no effect of particle length, or of length to diameter ratio on burning velocity.

Calculations of burning velocity were carried out using fuel and vapor properties as in reference 3. The transport properties of the gas were computed using the eddy viscosity model of reference 3 with turbulence intensity of 4% and a turbulence scale of 3 cm. Table 10 shows the results of the calculations. To calculate burning velocities which are sufficiently large for comparisons between the sprays tested, it was necessary to employ very rich mixtures for the sprays with very large diameter particles. For the 0.7% XD 8132.01 solution, the very large particles present resulted in no flame propagation for air-fuel ratios that are physically meaningful.

TABLE 10. CALCULATED VELOCITIES FOR FUELS USED
IN AIR SHEAR TESTS (REFERENCE 5)

Additive	Air/Fuel Ratio	Burning Velocity cm/sec.
Neat Jet A	3.79	40
0.2% AM-1	0.01	20
0.4% FM-4	2.5	23
0.7% XD 8132.01	-	Flame does not propagate

The results of this computation show that based on the particle size that was observed in reference 4, the mixtures tested can be classified as follows in terms of decreasing burning velocity at the same air-fuel ratio: Neat Jet-A, 0.4% FM-4, 0.2% AM-1, and 0.7% XD 8132.01.

CONCLUSIONS

Measurement of particle size distributions and air-fuel ratios in liquid fuel sprays was carried out using a Fraunhofer holographic technique. The sprays were generated in the laboratory, and the liquid fuel used was Neat Jet-A. The measured droplet size distributions were represented using Upper-Limit Log-Normal distribution parameters. The Sauter mean diameter, maximum droplet diameter, and total spray mass calculated from the distributions were in agreement with the experimental data. It was shown that the holocamera can be employed in daylight, so that holograms of modified fuel sprays during field tests appear feasible.

Burning velocity measurements in neat Jet-A sprays were in good agreement with calculated predictions using the one-dimensional spray model previously developed under the present contract. It can, therefore, be concluded that this model is capable of calculating burning velocities, and of predicting the expected variation of burning velocity as a function of the various spray parameters, at least for fuels where the physiochemical properties can be reasonably well approximated.

Particles in modified fuel sprays produced by air shear in a wind tunnel were approximated using a mean diameter and a mean length to diameter ratio. Using photographs of such sprays particle sizes from three modified fuels, as well as Jet-A, were employed for burning velocity calculations, and for rating the fuels with respect to burning velocity.

Using the laboratory equipment employed for neat Jet-A, it was not possible to generate modified fuel sprays sufficiently rich for burning velocity measurements.

RECOMMENDATIONS

Since modified fuels result in sprays with non-spherical particles, it is recommended that experimental work be undertaken for the study of the burning behavior of such particles singly, and in sprays. In the latter case, measured burning velocities should be correlated with particle sizes and shapes.

The ultimate fate of the stringlike and membranous particles in modified fuel sprays is a function of relaxation time as the particles accelerate, and as the shearing action between the particles and the ambient gas decreases. These particles could collapse to droplets if the fluid relaxation is shorter than the time for the fluid to hit the ground, or an obstacle. It is, therefore,

recommended to carry out an experimental study to measure particle
sizes during the whole lifetime of the spray, from the initiation
of the spill to the time that the liquid hits the ground. Such a
study would shed light on the antimisting behavior of modified
fuels during a crash, even during the time that the fuel mist is
behind the aircraft, and would help in the interpretation of crash
results.

REFERENCES

1.   Polymeropoulos, C. E., "Flame Propagation in a One-Dimensional Liquid Fuel Spray," Comb. Sci. Tech., 9, p. 197, (1974).

2.   Polymeropoulos, C. E., and Das, S., "The Effect of Droplet Size on the Burning Velocity of Kerosene-Air Sprays," Combustion and Flame, 25, p. 247 (1975).

3.   Polymeropoulos, C. E., "Ignition and Propagation Rates in a Fuel Mist," Interim Report, No. FAA-RD-75-155, October, 1975.

4.   Zinn, S. V., Eklund, T. I., and Neese, W. E., "Photographic Investigation of Modified Fuel Disintegration and Ignition," Final Report, No. FAA-RD-76-109, September 1976.

5.   Burgoyne, J. H., and Cohen, L., "The Effect of Drop Size on Flame Propagation in Liquid Aerosols," Proc. Roy. Soc. of London, 225, p. 375, (1954).

6.   Mizutani, Y., and Nishimato, T., "Turbulent Flame Velocities in Premixed Sprays, Part I - Experimental Study," Comb. Sci. and Tech., 6, p. 1 (1972).

7.   Ingebo, R. D., "Vaporization Rates and Drag Coefficients for Iso-Octae Sprays in Turbulent Air Streams," NACA TN 3265, 1954.

8.   Rice, E. T., "The Effect of Selected Fluid Parameters on Spatial Drop Size," Ph.D. Thesis, University of Wisconsin, 1966.

9.   Thompson, B. J., Ward, J. H., and Zinky, W. R., "Application of Hologram Techniques for Particle Size Analysis," Applied Optics, 6, p. 519 (1967).

10.   Kurtz, R. L., "The Techniques of Holographic Particle Sizing," NASA TR R-404, 1973.

11.   Polymeropoulos, C. E., Sernas, V., Jones, D., Veninger, A., "Generation of Polydisperse Sprays for Combustion Studies," Presented at the Eastern States Section of the Combustion Institute Meeting, Stony Brook, November, 1975.

12.   Silverman, B. A., and Thompson, B. J., "A Laser Fog Disdometer," J. Appl. Meterology, 3, p. 792 (1964).

13.   Mugele, R. A., and Evans, H. D., "Droplet Size Distribution in Sprays," Ind. Eng. Ch., 43, p. 1317 (1951).

14.   Allen, T., "Particle Size Measurement," Chapman and Hall, London, 1968, p. 66.

15.   Massey, F. J., Jr., "The Kolmogorov-Smirnov Test for Goodness of Fit," J. Am. Stat. Assoc., 46, p. 70 (1951).